COMPLEX WISHART DISTRIBUTION-BASED CHANGE DETECTION WITH POLARIMETRIC TERRASAR-X IMAGERY

Frank Thonfeld[1], Allan A. Nielsen[2], Henning Skriver[2], Knut Conradsen[3] & Morton J. Canty[1,4]

[1] *University of Bonn, Center for Remote Sensing of Land Surfaces (ZFL), D-53113 Bonn, Germany, frank.thonfeld@uni-bonn.de*
[2]*Technical University of Denmark, DTU Space – National Space Institut, DK-2800 Kgs. Lyngby, Denmark*
[3]*Technical University of Denmark, DTU Informatics – Department of Informatics and Mathematical Modelling, DK-2800 Kgs. Lyngby, Denmark*
[4]*Research Center Jülich, Institute for Bio- and Geosciences, D-52425 Jülich, Germany*

ABSTRACT

In this contribution, we present a change detection method based on the complex Wishart distribution. A maximum likelihood estimate for the complex covariance matrix of the distribution can be realized. In case that the components of the matrix are not independent and identically distributed, the so-called equivalent number of looks (ENL) may be used to parameterize the distribution. For two co-registered, look-averaged polarimetric images acquired at times t_1 and t_2, a per-pixel, generalized likelihood ratio test for equal covariance matrices has a critical region, assumed to be the same for both images. The associated asymptotic probability of obtaining a smaller value of the test statistic is given in the maximum likelihood estimate for the complex covariance matrix, so that the decision threshold can be chosen for any desired confidence level. In this contribution we illustrate a change detection procedure applicable to single, dual and quad polarimetric TerraSAR-X images and examine its sensitivity to the ENL parameter.

1 Introduction

Many methods based on SAR data have been developed to detect changes on the ground over time. Although the term change detection is widely used for land cover and land use change related applications, moving targets such as glaciers, landslides, or subsiding buildings may be detected by means of SAR likewise. However, those applications are generally not considered in terms of change detection. In fact, they reflect changes on the ground and must not be neglected in change detection surveys. Change detection methods measure the difference between two or multiple images. Well known methods based on phase information comprise interferometric SAR (InSAR) coherence difference [1], persistant scatterer interferometry (PSI) [2], or differential interferometry (DInSAR) [3]. Methods based on SAR amplitude comprise differential radargrammetry [4], image ratioing [5], or feature tracking [6]. Some recent advances were made by means of transformations such as curvelets [7]. Most common SAR change detectors work with univariate methods using only one polarization. In the case of dual or quad polarimetric data these methods require pre-selection of one image band, thereby ignoring information that could improve change estimation. Only few methods exist that make use of the polarimetric information [8], [9]. In [9], a test statistic based on the Wishart-distributed complex covariance matrix is presented. Here, we present a fully automatic method that makes use of the full polarimetric information of SAR images.

2 Methods

2.1 Complex Wishart distribution

The scattering amplitudes measured in a polarimetric SAR image in which horizontal and vertical polarized pulses are both emitted and detected may represented by the vector

$$s = (S_{hh}, S_{hv}, S_{vv})^\top,\ S_{hv} = S_{vh}\ \text{(reciprocity)} \qquad 1$$

which is often assumed to be zero-mean, complex multivariate normally distributed [10]. A maximum likelihood estimate for the complex covariance matrix of the distribution is given by

$$\hat{\Sigma} = \frac{1}{m} X = \frac{1}{m} \sum_{i=1}^{m} s_i s_i^{\dagger}, \qquad m \geq 3 \qquad 2$$

The quantity $\boldsymbol{x}$ in Equation 2 is a realization of a random matrix having a complex Wishart distribution with m degrees of freedom, provided that the $\boldsymbol{s}_i$, i = 1…m, are independent and identically distributed (i.i.d):

$$\langle \boldsymbol{C} \rangle = \begin{bmatrix} \langle S_{hh} S_{hh}^* \rangle & \langle S_{hh} S_{hv}^* \rangle & \langle S_{hh} S_{vv}^* \rangle \\ \langle S_{hv} S_{hh}^* \rangle & \langle S_{hv} S_{hv}^* \rangle & \langle S_{hv} S_{vv}^* \rangle \\ \langle S_{vv} S_{hh}^* \rangle & \langle S_{vv} S_{hv}^* \rangle & \langle S_{vv} S_{vv}^* \rangle \end{bmatrix} \qquad 3$$

In a lookaveraged polarimetric SAR image in covariance matrix format (Equation 3), the pixels are provided in the form of the covariance matrix estimates given by Equation (2) and therefore, when multiplied by m, they are complex Wishart distributed. In general, however, the contributing observations are correlated and therefore not i.i.d. In that case, the so-called equivalent number of looks (ENL) may be used to parameterize the distribution. Usually, ENL is estimated from the image data themselves by manually selecting homogeneous regions and calculating the ENL as ratio of squared intensities I and variance of intensity:

$$ENL = \frac{\langle I \rangle^2}{var(I)} \qquad 4$$

Recently, a multivariate maximum likelihood estimator for ENL was proposed [11] which makes optimal use of the polarimetric observations.

2.2 Change detection procedure

To detect changes between two polarimetric SAR images, a generalized likelihood ratio test may be applied [9]. It is a per-pixel test statistic for equality of two complex Wishart-distributed covariance matrices X and Y of two quad polarimetric images acquired at times t_1 and t_2:

$$Q = 2^{6m} \frac{|X|^m |Y|^m}{|X+Y|^{2m}} \leq k \qquad 5$$

where $|\cdot|$ denotes determinant and m is the estimated ENL, assumed to be the same for both images. Q lies between 0 and 1 with 1 meaning total equality between the matrices. The associated asymptotic probability of obtaining a smaller value of the test statistic is given in [9], so that the decision threshold k can be chosen for any desired confidence level. The method makes use of the full polarimetric matrix but also works for dual polarimetric data. In the case of single polarization data the method reduces to a simple ratioing.

3 Data

In this contribution we illustrate the above change detection procedure with quad polarimetric TerraSAR-X images and examine its sensitivity to the ENL parameter. The images were acquired over an open pit lignite mining area near Cologne in the German province of North Rhine-Westphalia. Pre-processing comprised multilooking with 2x3 looks and georeferencing. Since no DEM taken at the same time was available geocoding was done to a constant reference height.

The quad polarimetric TerraSAR-X images were acquired during an experimental dual receive antenna phase on April 18th, April 29th, and May 10th, 2010. A RGB composite of the respective span images of a subset of 12x12 km² is shown in **Figure 1**. Grey level colors may interpreted as no-change areas with bright colors showing strong backscatter and dark areas showing weak backscatter. The most obvious changes - red, green and blue spots inside the pit – are due to the position of the large excavators and backfill machines at each respective date. The colored areas outside the pit show significant phenological changes of agricultural fields.

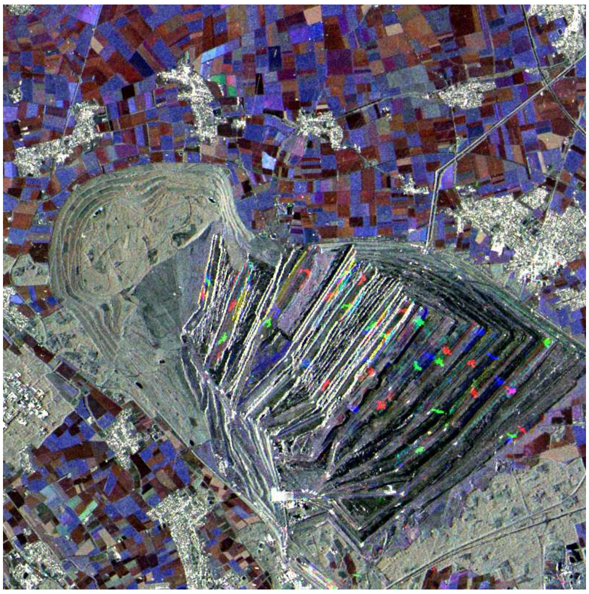

Figure 1 RGB composite of the span images taken on April 18th, April 29th and May 10th, 2010.

4 Results

Figure 2 is an ENL image for the April 18th, April 29th and May 10th, 2010 scenes and their histograms using the multivariate estimator of [11] calculated in a running 7×7 window. Villages and irregularities in the open pit area correspond to low values of ENL, due to the high variability of the radar cross sections within the window. In more homogeneous regions, the speckle statistics are well developed leading to a fairly uniform ENL. The histogram of the ENLs are also shown. Their mode is 4.9, 4.9, and 4.8, respectively.

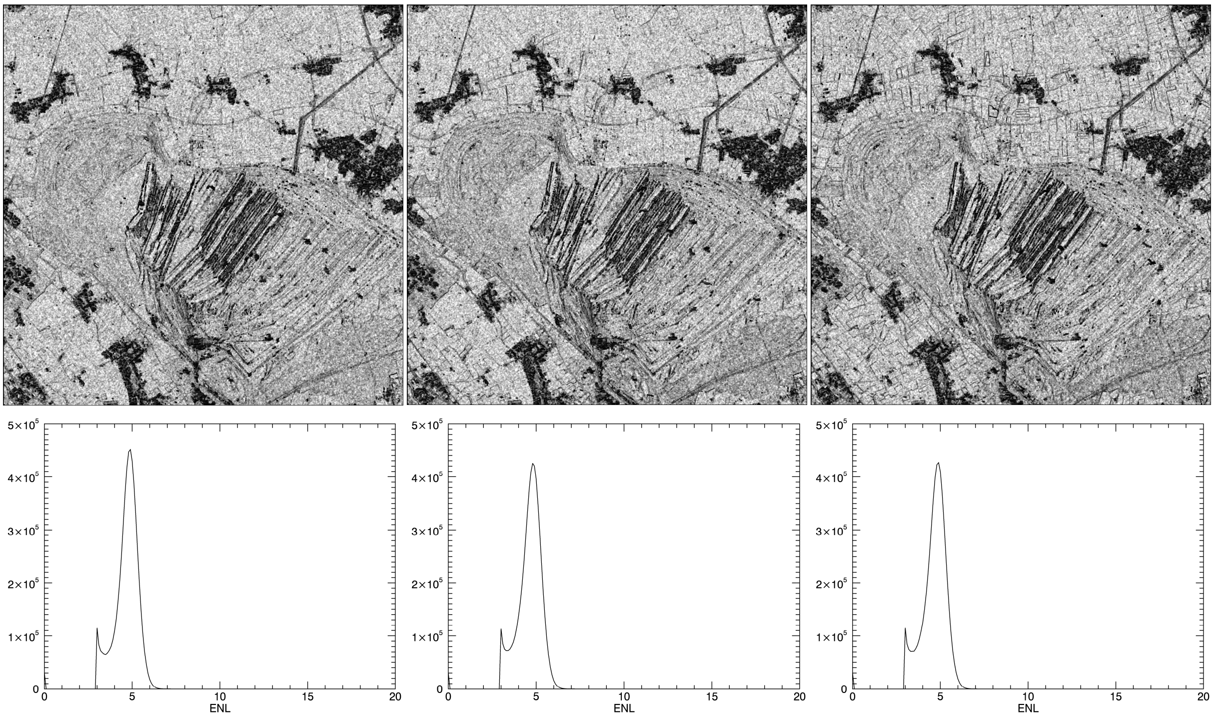

Figure 2 ENL images and histograms for April 18th (left), April 29th (mid) and May 10th, 2010 (right). The mode, i.e. the ENL estimated for the whole image, is 4.9, 4.9 and 4.8, respectively.

This value is considered to represent the ENL of the whole scene. With this value, the decision statistic Q, Equation (5), was determined.

Figure 3 shows the function $-2\rho\ln Q$, whose probability distribution is known asymptotically. **Figure 4** is the corresponding change probability image. Areas with highest probability of change are concentrated inside the open pit with the excavators, who changed their position, and the mined areas. Changes in agricultural fields are less pronounced. **Figure 5** shows the changes at the 1% confidence limit ($P(-2\rho\ln Q \leq z) \geq 0.99$). Again, the strongest changes are due to excavators and backfill machines changing their positions. The remaining changes, e.g. phenological changes of agricultural fields are below the 1% confidence interval.

The scalar definition of ENL, Equation (4), where I is intensity in a spatially homogeneous region of a single polarimetric band, gave estimates ranging from about 3 to 4 depending on region chosen. The effect of different ENL values on the change detection results is illustrated in **Figure 6**. The higher the ENL considered the higher the proportion of changes areas at the same confidence interval. This in turn means that a too low ENL value leads to underestimation and a too high ENL value leads to overestimation of

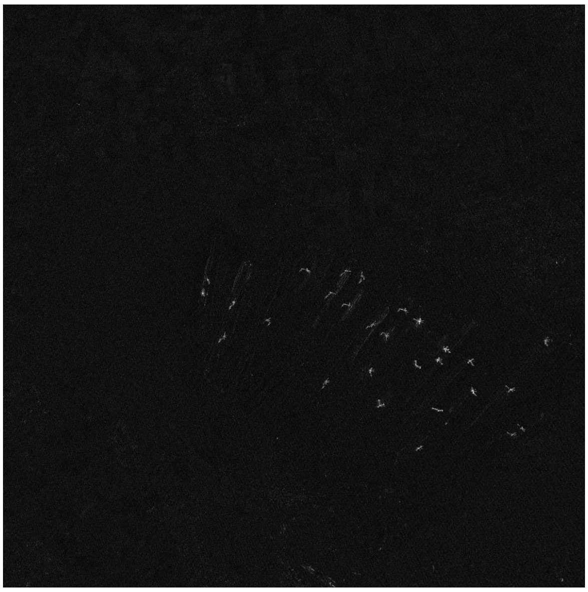

Figure 3 Likelihood ratio test statistic $-2\rho\ln Q$ (linear stretch) for changes between April 18th and May 10th.

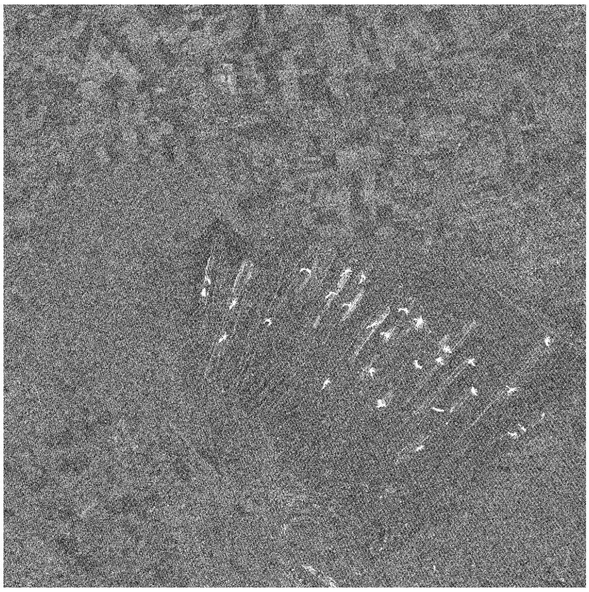

Figure 4 Change probability $P(-2\rho\ln Q \leq z)$ (linear stretch).

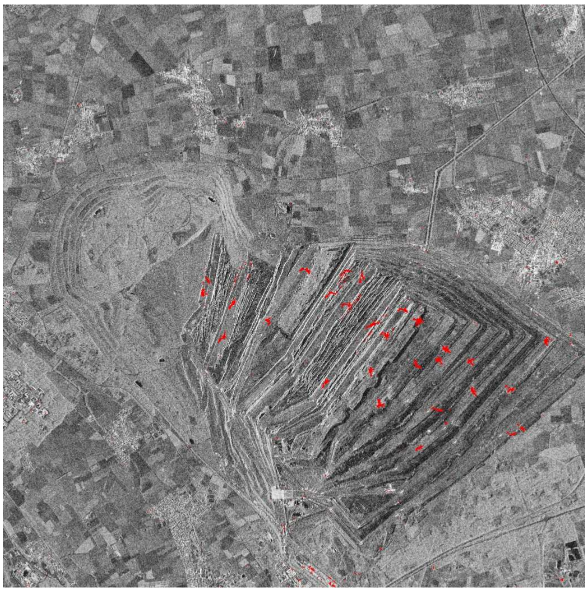

Figure 5 HH image overlaid with changes at 1% confidence level.

change areas. Validation of the change detection result is challenging. Although being an obvious change, the shifted positions of the excavators and backfill machines in the open pit could easily be detected.

Acknowledgment

The TerraSAR-X data used in this study were provided by DLR under AO MTH0822.

References

[1] Liao, M., L. Jiang, H. Lin, B. Huang & J. Gong. Urban Change Detection Based on Coherence and Intensity Characteristics of SAR Imagery. Photogrammetric Engineering & Remote Sensing 74 (8):999–1006, 2008.

[2] Ferretti, A., G. Savio, R. Barzaghi, A. Borghi, S. Musazzi, F. Novali, C. Prati & F. Rocca. Submillimeter Accuracy of InSAR Time Series: Experimental Validation. IEEE Transactions on Geoscience and Remote Sensing 45 (5):1142–1153, 2007.

[3] Bamler, R. & P. Hartl. Synthetic Aperture Radar Interferometry. Inverse Problems 14 (4):R1–R54, 1998.

[4] Polidori, L., S. Caillault & J.-L. Canaud. Change Detection in Radar Images: Methods and Operational Constraints. IEEE International Geoscience and Remote Sensing Symposium. IGARSS'95. "Quantitative Remote Sensing for Science and Applications", 2:1529–1531, 1995.

[5] Rignot, E. J. M. & J. J. Van Zyl. Change Detection Techniques for ERS-1 SAR Data. IEEE Transactions on Geoscience and Remote Sensing 31 (4):896–906, 1993.

[6] Strozzi, T., A. Luckman, T. Murray, U. Wegmuller & C. L. Werner. Glacier Motion Estimation Using SAR Offset-tracking Procedures. IEEE Transactions on Geoscience and Remote Sensing 40 (11):2384–2391, 2002.

[7] Schmitt, A., B. Wessel & A. Roth. Curvelet-based Change Detection on SAR Images for Natural Disaster Mapping. Photogrammetrie - Fernerkundung – Geoinformation 2010 (6): 463–474, 2010.

[8] Schmitt, A. Änderungserkennung in multitemporalen und multipolarisierten Radaraufnahmen. Dissertation, Karlsruher Institut für Technologie (KIT). http://digbib.ubka.uni-karlsruhe.de/volltexte/1000025955, 2012.

[9] Conradsen, K., A.A. Nielsen, J. Schou & H. Skriver. A test statistic in the complex Wishart distribution and its application to change detection in polarimetric SAR data. IEEE Transactions on Geoscience and Remote Sensing, 41(1):3-19, 2003.

[10] Oliver, C. & S. Quegan. Understanding Sythetic Aperture Radar Images. SciTech, 2004.

[11] Anfinsen, S., A. Doulgeris & T. Eltof. Estimation of the equivalent number of looks in polarimetric synthetic aperture radar imagery. IEEE Transactions on Geoscience and Remote Sensing, 47(11):3795-3809, 2009.

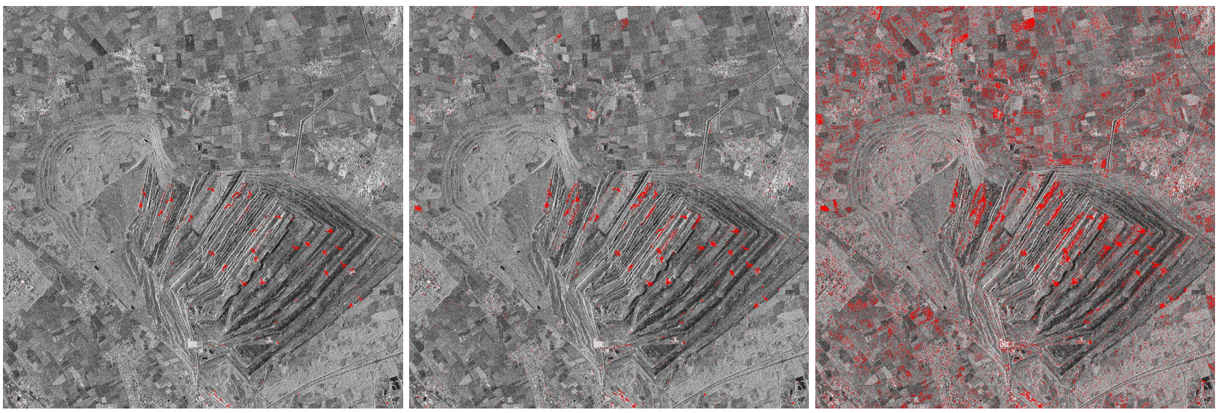

Figure 6 HH image overlaid with changes at 5% confidence level for ENL = 4.0 (left), ENL = 4.9 (mid) and ENL = 6.0 (right).